With the exception of the long storm of April 15, the average solar storm has a duration of 10 minutes and an amplitude of 120°K.

With the present low-gain antenna, a detailed account cannot be made of the sources of the solar radiations. However, some idea of a distribution was obtained from measurements taken during a partial eclipse of the sun on November 23, 1946.[15] On this day the measured temperature of the radiation resistance was 460°K. A sudden .9 per cent decrease of the solar noise occurred three minutes before the first contact. The spectroheliograms taken on November 24 and 25 by the Mount Wilson Observatory show an extensive band of prominences on the northern hemisphere, extending off the western limb just at the point of contact. It seems likely that a prominence existed on the day of the eclipse, so that the initial reduction of noise occurred when it was being obscured. The associated equivalent temperature of the prominence is of the order of 2×10^7°K. A further 25 per cent reduction was associated with the passage of the moon across a central region (2.2 per cent of the sun's projected surface) which contained a large sunspot. From the data obtained, an equivalent temperature of 1.5×10^6°K. was calculated for this area. A sharp fall and rise in the noise occurred with the covering and uncovering of the penumbra of the well-formed leading spot of the group.

[15] A. E. Covington, "Microwave solar noise observations during the partial eclipse of November 23, 1946," *Nature*, vol. 159, pp. 405–406; March 22, 1947.

An Analysis of the Intermodulation Method of Distortion Measurement*

W. J. WARREN†, SENIOR MEMBER, I.R.E., AND W. R. HEWLETT†, FELLOW, I.R.E.

Summary—**Part A of this paper is an analysis of the intermodulation method of distortion measurement. Results obtained by its use are compared with those obtained by the harmonic-measurement method. Predicted values for the intermodulation distortion and harmonic distortion are given for several typical transfer characteristics. For single-ended and push-pull characteristics, which are representable by simple power series, general equations are derived for intermodulation and harmonic distortion. With the aid of equations for the former, the effects of the ratio of signal amplitudes used in intermodulation testing are studied. These equations also permit derivation of relatively fixed ratios of per cent intermodulation distortion to per cent harmonic distortion for an intermodulation test method, which is described. Predicted values for distortion and their ratios are supported by test results. Curves expressing the actual distortion ratios, plotted against harmonic distortion, summarize the results of this analysis. These curves are useful for correlating the results of the two methods of test. Possible meter types, usable for metering the carrier- and intermodulation-frequency components in the intermodulation test method, are reviewed. The choice of meter type is found to affect the readings obtained for these components, and hence will affect the per cent intermodulation distortion. In Part B, simple equations are given for approximate predetermination of per cent intermodulation distortion from three or five points on the transfer characteristic. For more accurate prediction, tables are given for calculation of the prominent intermodulation components from eleven points on the transfer characteristics.**

Introduction

THE INTERMODULATION METHOD of distortion measurement[1–3] has been receiving increasing attention in the last few years. Instruments have been developed for application of this method. The question: "How will results obtained by the intermodulation method compare with those of harmonic measurement?" has been asked frequently. To provide an answer to this question, the intermodulation method is analyzed in this paper, and results are presented comparing the two methods. The comparisons will hold for test conditions for which both methods are applicable.

The analysis is based on the fact that the same nonlinearity of the transfer characteristic of a network that causes harmonic distortion also causes intermodulation distortion. The extent to which the transfer characteristic is nonlinear may vary with frequency, as in disk reproduction. This paper assumes that the transfer characteristic is substantially independent of frequency. Then, the sameness of the underlying factors causing distortion leads to the development of relatively fixed ratios for per cent intermodulation to per cent harmonic distortion. For the intermodulation test method described below, this ratio is about 3.2 to 1 for a single-ended amplifier and about 3.8 to 1 for a balanced push-pull amplifier.

Several methods have been proposed for intermodulation testing, and, to differing extents, most of these

* Decimal classification: R225.12×R148.18. Original manuscript received by the Institute, June 10, 1947; revised manuscript received October 8, 1947. Presented, National Electronics Conference, November, 1947, Chicago, Ill.

† Hewlett-Packard Co., Palo Alto, Calif.

[1] D. C. Espley, "Harmonic production and cross modulation in thermionic values with resistive loads," PROC. I.R.E., vol. 22, pp. 781–791; June, 1934.

[2] John K. Hilliard, "Distortion measurements by the intermodulation method," PROC. I.R.E., vol. 29, pp. 614–620; December, 1941.

[3] H. H. Scott, "Audible audio distortion," *Electronics*, vol. 18, p. 126; January, 1945.

are in use.[1–5] This paper will confine itself to an analysis of one of the generally accepted methods.[5] Similar analyses can be made for each method; giving rise to specific numeric relations, as illustrated above, for each method. A block diagram of the intermodulation test method being treated is shown in Fig. 1, and the principle of operation is described below.

For brevity, harmonic distortion will hereafter be written *HD* and intermodulation distortion will be written *IM*.

The signal frequencies used in *IM* testing are chosen so f_b (Fig. 1) is higher than f_a, and their actual values are selected with regard to the frequencies at which performance of the test unit is to be examined, and with regard to the frequency characteristics of the filters used. Typical values for the *IM* method being treated are 40, 60, and 100 cycles for f_a, and 1000, 7000, and 12,000 cycles for f_b. Present practice makes the high-frequency signal (V_b) 12 db lower than the low-frequency signal V_a. The effect of this voltage ratio upon the quantitative results obtained is discussed in a subsequent section.

The *IM* apparatus is calibrated by introducing two signals at X-X', or Y-Y', in Fig. 1; one of frequency f_a' and of magnitude V_a', and the other of frequency f_b' and magnitude V_b'. These voltages and frequencies are so selected that $V_a' = 10\,V_b'$, $f_b' - f_a'$ is in the pass band of the low-pass filter, while both f_a' and f_b' are greater than the cutoff frequency of the high-pass filter. The envelope of the composite signal, $V_a' + V_b'$, will be nearly sinusoidal and of amplitude B_b' with apparent carrier level nearly equal to V_a'.[6] The results of detection and metering will give a reading on the output meter M' proportional to V_b', and a reading on the carrier meter M_c proportional to V_a'. Since the amplitude ratio B_b' to V_a' is 0.1, the ratio of output-meter to carrier-meter readings is, by definition, 10 per cent intermodulation. In actual practice, an amplifier with adjustable gain is used ahead of the carrier meter M_c to set this meter to a 100 per cent mark. This permits calibration of the output meter M' directly in per cent *IM*.

Part A—Analysis of Intermodulation Method and Comparison with Harmonic-Distortion Method

Scope of Analysis

For quantitative comparison of the *IM* and *HD* techniques and to evaluate the effects of metering practice in the former, the following cases have been treated:

I. Transfer characteristic readily representable by a power series.

II. Transfer characteristic having an abrupt slope change, for which case the power series becomes too lengthy for convenient treatment.

III. Transfer characteristic representable by a portion of a sine wave.

The analysis and comparisons assume that:

1. The transfer characteristic is independent of frequency. Many applications of the test methods considered will satisfy this assumption wholly or reasonably well. An exception, disk reproduction, was previously cited.

2. The same total peak driving voltage is used for both methods of test. The device under test will thereby be working between the same limits of input voltage and output current. If the same total output power is used as a basis of comparison, the peak driving voltage, with a signal of two or more frequencies, would be larger than the peak single-frequency voltage by an amount depending upon the ratio of signal-voltage amplitudes.

In their respective cases, per cent harmonic distortion and per cent intermodulation distortion are respectively evaluated according to the definitions:

$$\text{per cent r.m.s. } HD = \frac{\sqrt{\sum (\text{harmonic output voltages, or currents})^2}}{\text{fundamental output voltage, or current}} \times 100 \quad (1)$$

and

$$\text{per cent r.m.s. } IM = \frac{\sqrt{\sum (\text{sum and difference frequency voltages in output})^2}}{\text{fundamental output voltage of one of the signals}} \times 100. \quad (2)$$

In (1) a sine-wave signal voltage is assumed, and in (2) the two signals are both assumed sinusoidal. Unless specifically noted otherwise, in this paper per cent *HD* and per cent *IM* will denote the r.m.s. values.

Case (I-a). Power Series for Single-Ended Transfer Characteristic: The transfer characteristic of a nonlinear network or amplifier may be represented by a power series in which the output current may be expressed as a function of increasing powers of input voltage. Thus

$$i = a_0 + a_1 e + a_2 e^2 + a_3 e^3 + \cdots + a_n e^n \quad (3)$$

and

$$e = A_0 + A \sin a \pm B \sin b; \quad (4)$$

then, considering only terms up to and including the 5th-power term,

$$i = \text{d.c. component} + A\{a_1 + 2a_2A_0 + 3a_3(A_0^2 + \tfrac{1}{4}A^2 + \tfrac{1}{2}B^2) + 4a_4(A_0^3 + \tfrac{3}{4}A_0A^2 + \tfrac{3}{2}A_0B^2) + 5a_5(A_0^4 + \tfrac{3}{2}A_0^2A^2 + 3A_0^2B^2 + \tfrac{3}{4}A^2B^2 + \tfrac{3}{8}B^4 + \tfrac{1}{8}A^4)\} \sin a$$

$$- A^2\left\{\frac{a_2}{2} + \frac{3a_3}{2}A_0 + a_4(3A_0^2 + \tfrac{1}{2}A^2 + \tfrac{3}{2}B^2)\right.$$

[4] N. C. Pickering, "Measuring audio intermodulation," *Electronic Ind.*, vol. 5, pp. 55–58; June, 1946.

[5] John K. Hilliard, "The use of intermodulation tests in designing and selecting high quality audio channels," Altec-Lansing Corp., Hollywood, Calif., issue no. 2, May, 1946.

[6] F. E. Terman, "Radio Engineer's Handbook," McGraw-Hill Publishing Co., New York, N. Y., 1943; p. 567.

$$+5a_5(A_0^3+\tfrac{1}{2}A_0A^2+\tfrac{3}{2}A_0B^2)\Big\}\cos 2a$$
$$-A^3\{\tfrac{1}{4}a_3+a_4A_0+5a_5(\tfrac{1}{2}A_0^2+\tfrac{1}{4}B^2+\tfrac{1}{16}A^2)\}\sin 3a$$
$$+\tfrac{1}{8}A^4\{a_4+5a_5A_0\}\cos 4a+\tfrac{1}{16}a_5A^5\sin 5a$$
$$\pm B\{a_1+2a_2A_0+3a_3(A_0^2+\tfrac{1}{4}B^2+\tfrac{1}{2}A^2)$$
$$+4a_4(A_0^3+\tfrac{3}{4}A_0B^2+\tfrac{3}{2}A_0A^2)+5a_5(A_0^4+\tfrac{3}{2}A_0^2B^2$$
$$+3A_0^2A^2+\tfrac{3}{4}A^2B^2+\tfrac{3}{8}A^4+\tfrac{1}{8}B^4)\}\sin b$$
$$\pm AB\{a_2+3a_3A_0+3a_4(2A_0^2+\tfrac{1}{2}A^2+\tfrac{1}{2}B^2)$$
$$+5a_5(2A_0^3+\tfrac{3}{2}A_0A^2+\tfrac{3}{2}A_0B^2)\}[\cos(b-a)-\cos(b+a)]$$
$$\mp A^2B\{\tfrac{3}{4}a_3+3a_4A_0+5a_5(\tfrac{3}{2}A_0^2+\tfrac{3}{4}A^2$$
$$+\tfrac{3}{8}B^2)\}[\sin(b-2a)+\sin(b+2a)]$$
$$\mp A^3B\{\tfrac{1}{2}a_4+\tfrac{5}{2}a_5A_0\}[\cos(b-3a)-\cos(b+3a)]$$
$$\pm\tfrac{5}{16}a_5A^4B[\sin(b-4a)+\sin(b+4a)]$$
$$-B^2\Big\{\frac{a_2}{2}+\tfrac{3}{2}a_3A_0+a_4(3A_0^2+\tfrac{1}{2}B^2+\tfrac{3}{2}A^2)$$
$$+5a_5(A_0^3+\tfrac{1}{2}A_0B^2+\tfrac{3}{2}A_0A^2)\Big\}\cos 2b$$
$$+AB^2\{\tfrac{3}{4}a_3+3a_4A_0+5a_5(\tfrac{3}{2}A_0^2+\tfrac{3}{8}A^2$$
$$+\tfrac{3}{4}B^2)\}[\sin(2b-a)-\sin(2b+a)]$$
$$+A^2B^2(\tfrac{3}{4}a_4+\tfrac{15}{4}a_5A_0)[\cos(2b-2a)+\cos(2b+2a)]$$
$$-\tfrac{5}{8}a_5A^3B^2[\sin(2b-3a)-\sin(2b+3a)]$$
$$\pm B^3\Big\{\frac{a_3}{4}+a_4A_0+5a_5(\tfrac{1}{2}A_0^2+\tfrac{1}{4}A^2+\tfrac{1}{16}B^2)\Big\}\sin 3b$$
$$\mp AB^3\Big\{\frac{a_4}{2}+\tfrac{5}{2}a_5A_0\Big\}[\cos(3b-a)-\cos(3b+a)]$$
$$\pm\tfrac{5}{8}a_5A^2B^3[\sin(3b-2a)+\sin(3b+2a)]$$
$$+\tfrac{1}{8}B^4(a_4+5a_5A_0)\cos 4b$$
$$-\tfrac{5}{16}a_5AB^4[\sin(4b-a)-\sin(4b+a)]$$
$$\pm\tfrac{1}{16}a_5B^5\sin 5b. \qquad (5)$$

Equation (5) reduces to the output current for *IID* measurement upon setting $B=0$.

Terms involving f_b and its harmonics are grouped with corresponding sideband terms in (5). The high-pass filter (Fig. 1) removes all low-frequency terms, so that, if $f_b > 9f_a$, then all of the sidebands and carrier components will appear at the detector input, and all harmonics of f_a will be suppressed. The term of frequency f_b will predominate and the carrier-level meter, M_c, which is an average-reading meter, will indicate substantially only the amplitude of this term.

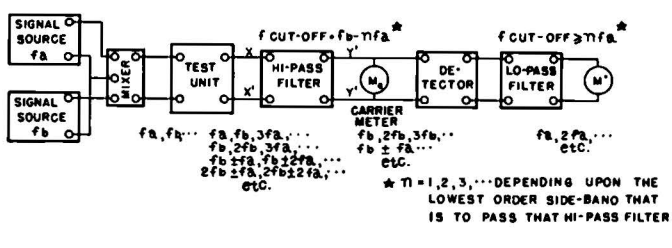

Fig. 1—Block diagram for intermodulation test method treated in this paper for calibration, f_a, f_b are connected into X-X' or Y-Y'.

Carrier and sideband term magnitudes in (5) are seen to depend upon the signal amplitudes A and B. For an assigned peak driving voltage and given quiescent status of an amplifier, the per cent *IM* will hence depend upon the ratio A/B. The exact nature of this dependence is partially discernible for the case of a transfer characteristic given by

$$i = a_1e + a_2e^2 + a_3e^3 + a_4e^4. \qquad (6)$$

With the origin for the characteristic taken at the operating point, i.e., $a_0=0$ and $A_0=0$, the signal for *IM* testing will be $e=A\sin a \pm B\sin b$, and for *HD* testing it will be $e=A'\sin a$. Applying the defining equations (1) and (2), there follows:

per cent *IM*

$$\cong 2A\frac{\{[a_2+\tfrac{3}{2}a_4(A^2+B^2)]+\tfrac{9}{16}a_3^2A^2+\tfrac{1}{4}a_4^2A^4\}^{1/2}}{a_1+\tfrac{3}{4}a_3(2A^2+B^2)}\times 100, \qquad (7a)$$

and

per cent *IID*

$$\cong\frac{A'}{2}\frac{\{[a_2+a_4(A')^2]+\tfrac{1}{4}a_3^2(A')^2+\tfrac{1}{16}a_4^2(A')^4\}^{1/2}}{a_1+\tfrac{3}{4}a_3(A')^2}\times 100. \qquad (8a)$$

If $A+B=A'$ for the same total peak driving voltage, $A/B=4$, and the usual insignificance of the squared values of a_3 and a_4 as compared to a_1^2 and a_2^2 is acknowledged, then

$$\text{per cent } IM \cong \frac{8}{5}\frac{A'(a_2+a_4(A')^2)}{a_1+a_3(A')^2}\times 100 \qquad (7b)$$

$$\text{per cent } IID \cong \frac{1}{2}\frac{A'(a_2+a_4(A')^2)}{a_1+\tfrac{3}{4}a_3(A')^2}\times 100. \qquad (8b)$$

When a_3 and a_4 are set equal to zero, (7b) and (8b) check those developed by Frayne and Scoville.[7] Equation (7a) indicates that, to a first approximation, the per cent *IM* will vary directly with the larger signal amplitude A. Maintaining the peak drive $A+B$ constant, it follows that, as A/B is increased, the per cent *IM* will approach a maximum. Comparison of (7b) and (8b) shows that, for the conditions imposed, *i.e.*, $A/B=4$, the theoretical ratio of per cent *IM* to per cent *HD* is practically constant at 3.2. A summary of the values of this ratio for several types of transfer characteristics is given in Fig. 15.

To check the above theory, a triode-connected 6V6 amplifier working into a 7500-ohm resistive load was tested. The dynamic characteristic for the chosen operating conditions was:

[7] J. G. Frayne and R. R. Scoville, "Analysis and measurements of distortion in variable-density recording," *Jour. Soc. Mot. Pic. Eng.*, vol. 32, p. 648; June, 1939.

$$i = 60 + 1.2423e + 0.0102e^2 + 0.972 \times 10^{-4}e^3$$
$$= 60(1 + 0.5383x + 0.1149x^2 + 0.0285x^3) \quad (9)$$

where i is in milliamperes, and $x = e/26$; *i.e.*, x is the fraction of the maximum peak drive of 26 volts. The coefficients in the equation, of the form of (3), were reduced from experimental data.

The effect of the ratio A/B of signal voltages upon the per cent IM and correlation between theoretical and experimental values is shown in Fig. 2. For a fixed

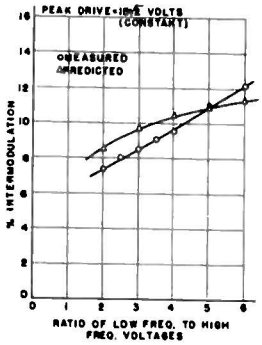

Fig. 2—Per cent intermodulation as a function of the ratio of signal amplitudes. Single-ended 6V6 amplifier; 7500-ohm load; bias voltage, 26 volts; plate-supply voltage, 610 volts.

ratio $A/B = 4$, the predicted and measured values for per cent IID and per cent IM agree well, as shown in Fig. 3. The agreement between per cent IM values obtained with an average-reading meter used for the output meter M' (Fig. 1) and those computed from data obtained with a harmonic analyzer at the output-meter position justifies the use of the former for measurement of the r.m.s. value of the complex output voltage.

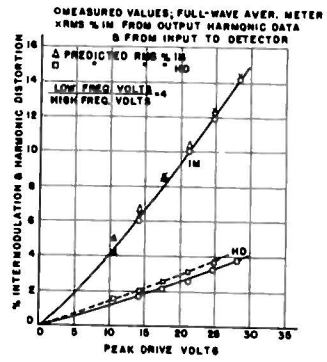

Fig. 3—Per cent intermodulation and harmonic distortion of the single-ended 6V6 amplifier of Fig. 2 as a function of signal voltage.

If the output meter M' is a full-wave, peak-reading meter, then the per cent IM, for the same conditions applying to (7a), will become:

per cent peak IM

$$= 2A \frac{[a_2 + \frac{3}{4}a_3A + \frac{1}{2}a_4(4A^2 + B^2)]}{a_1 + \frac{3}{4}a_3(2A^2 + B^2)} \times 100. \quad (10a)$$

The arithmetic summation of the sideband components is correct because of their relative phase relationships, as shown in Fig. 12. Relative magnitudes of the several components are such that, for all practical cases, the resultant peak is time-coincident with the peak of the fundamental. For $A+B=A'$, i.e., the same peak driving voltage for IM and IID testing, and $A/B=4$, (10a) becomes

per cent peak IM

$$= \frac{8}{5}A' \frac{[a_2 + \frac{3}{5}a_3A' + \frac{5}{4}a_4(A')^2]}{a_1 + \frac{99}{100}a_3(A')^2} \times 100. \quad (10b)$$

In like manner, measurement of harmonic distortion by a full-wave peak-reading meter will give

per cent peak HD

$$= \frac{A'}{2} \frac{[a_2 + \frac{1}{2}a_3A' + \frac{5}{4}a_4(A')^2]}{a_1 + \frac{3}{4}a_3(A')^2} \times 100. \quad (11)$$

Comparison of (10b) and (11) reveals that the ratio of peak per cent IM to peak per cent IID will again remain practically constant at 3.2.

Case (I-b). Power Series for Push-Pull Transfer Characteristic: All terms involving a_0, A_0, a_2, and a_4 in (5) vanish for the perfectly balanced push-pull amplifier. The effect of signal voltage ratio A/B upon per cent IM and per cent HD is partially discernible upon applying the defining equations (1) and (2) to the applicable form of (5). There results:

per cent IM

$$\cong \frac{3A^2}{2} \frac{\{[a_3 + \frac{5}{2}a_5(2A^2 + B^2)]^2 + (\frac{5}{12}a_5A^2)^2\}^{1/2}}{a_1 + \frac{3}{4}a_3(2A^2 + B^2) + \frac{15}{8}a_5(2A^2B^2 + 3B^4 + A^4)} \times 100 \quad (12a)$$

and

per cent HD

$$\cong \frac{(A')^2}{4} \frac{\{[a_3 + \frac{5}{4}a_5(A')^2]^2 + (\frac{1}{4}a_5(A')^2)^2\}^{1/2}}{a_1 + \frac{3}{4}a_3(A')^2 + \frac{5}{8}a_5(A')^4} \times 100. \quad (13a)$$

For given operating conditions and constant peak signal voltage, (12a) indicates that per cent IM will vary roughly as the square of the larger signal amplitude A. Typical push-pull characteristics will often have a negative value for the coefficient a_3. This tends to make the variation of per cent IM with signal ratio to be somewhat more rapid than as A^2. For $A/B=4$ and $A+B=A'$, and neglecting the usually small terms, (12a) and (13a) become

$$\text{per cent } IM \cong \frac{24}{25}(A')^2 \frac{[a_3 + \frac{33}{10}a_5(A')^2]}{a_1 + a_3(A')^2} \times 100 \quad (12b)$$

and

$$\text{per cent } HD \cong \frac{1}{4}(A')^2 \frac{[a_3 + \frac{5}{4}a_5(A')^2]}{a_1 + \frac{3}{4}a_3(A')^2} \times 100, \quad (13b)$$

resulting in a ratio of IM to HD which is practically

3.84. The effect of a negative a_3 is to make this ratio increase with peak-signal level A'. If the terms involving a_5 in the numerator and a_3 in the denominator are neglected, then (12b) and (13b) agree with those given by Frayne and Scoville[7] for the cubic characteristic.

If the output meters M' and M_c are full-wave peak-reading meters, then the per cent IM and IID become, respectively, by the method of analysis used with (10) and (11),

per cent peak IM

$$\cong \frac{24}{25}(A')^2 \frac{[a_3 + \tfrac{107}{30}a_5(A')^2]}{a_1 + \tfrac{39}{100}a_3(A')^2 + \tfrac{873}{1000}a_5(A')^4} \times 100 \quad (14)$$

and

per cent peak IID

$$\cong \frac{1}{4}(A')^2 \frac{[a_3 + \tfrac{3}{2}a_5(A')^2]}{a_1 + \tfrac{3}{4}a_3(A')^2 + \tfrac{5}{8}a_5(A')^4} \times 100. \quad (15)$$

It is seen that the ratio of per cent peak IM to per cent peak IID will be nearly constant at 3.84.

The absence of even-harmonic carrier-frequency terms eliminates the detector turnover effect discussed in connection with Fig. 13. Even-order harmonics of the principal output low frequency $2f_a$ may, however, prevail at the meter M'.

For experimental verification, a push-pull 6L6 amplifier was tested. The dynamic characteristic for the 8000-ohm plate-to-plate load was representable by

$$i = 2.567e - 0.1207 \times 10^{-3}e^3 - 0.66 \times 10^{-7}e^5$$
$$= 97.546(1 - 0.0679x^3 - 0.0332x^5), \quad (16)$$

where i is in ma. and $x = e/38$; i.e., x is the fraction of the maximum peak driving volts. The predicted per cent IM variation with signal ratio A/B and the measured

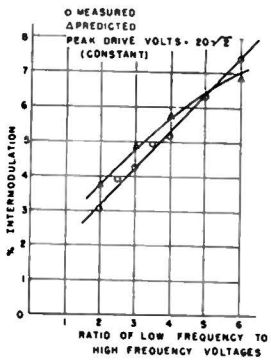

Fig. 4—Per cent intermodulation as a function of the ratio of signal amplitudes. Push-pull 6L6 amplifier; 8000-ohm plate-to-plate load; plate-supply voltage, 400 volts; bias voltage, 37 volts.

results are shown in Fig. 4. For the signal ratio $A/B = 4$, the measured and predicted per cent IM and per cent IID values, as a function of drive, are shown in Fig. 5. The measured results were independent of the direction of connection of the half-wave peak detector used. Though not shown, the results for per cent IM, obtained with a peak-reading output meter M', depended upon the direction of its connection because of the even-harmonic content of the low-frequency output.

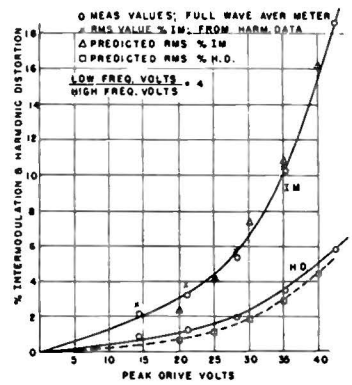

Fig. 5—Per cent intermodulation and harmonic distortion of the push-pull 6L6 amplifier of Fig. 4 as a function of signal voltage.

Case (II-a). Single-Ended, Sharp-Cutoff Characteristic: To simulate certain types of amplifier characteristics, such as that of an amplifier overdriven from a high-impedance source, or an amplifier having negative feedback that is driven beyond cutoff, the *e-i* characteristic shown in Fig. 6 was investigated. Insomuch as adequate

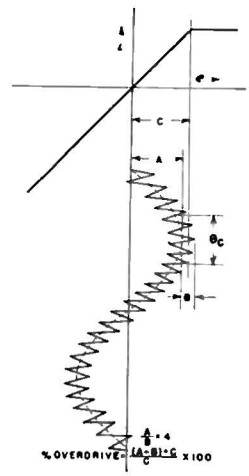

Fig. 6—Single-ended, sharp-cutoff characteristic with a two-frequency input signal.

representation by a power series requires too many terms, a different method of analysis was used. The steps in the approximate analysis were as follows:

1. For an arbitrary ratio f_a/f_b and signal ratio $A/B = 4$, the number of peaks "clipped" and the amplitude of each was determined for an assigned amount of overdrive. (See Fig. 6 for definition of overdrive.)

2. The total area under the clipped peaks was evaluated from their relative amplitudes and time-axis spans. (See Fig. 7(b).)

3. The half sine wave of Fig. 7(c) was so proportioned that its duration θ_c was equal to that clipped from the composite envelope, and its height so selected that the area under it was equal to that of the clipped peaks.

4. The reading of a full-wave average-reading meter, on which the wave of paragraph 3 is impressed, was

evaluated. This meter reading, compared to that of the same meter with only the carrier impressed, is the intermodulation distortion.

5. In actual testing, the carrier-level meter M_c has the wave of Fig. 7(a) impressed upon it. The reading

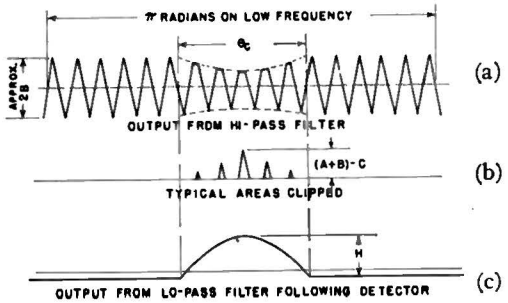

Fig. 7—Wave shapes applying to the analysis of the output current of the characteristic of Fig. 6.

of M_c will be less than if the carrier alone were impressed. For an average-reading meter, as used in the test arrangement for checking this analysis, the reading of M_c will be less, substantially, by the amount of the total areas clipped; i.e., by the amount corresponding to the area calculated in 2. The intermodulation distortion of paragraph 4 was corrected for this "carrier loss" to permit ready comparison with measured values.

6. For calculating the per cent *HD*, the procedure of steps 2 and 3 was repeated for the area clipped from the single signal wave. The fundamental frequency component of this wave was calculated and subtracted. The reading of an average-type meter, having the remaining wave impressed upon it, was determined and compared with the reading of the meter with the "unclipped" signal applied.

For a specific value of overdrive, the clipped areas of Fig. 7(b) were resolved by Fourier analysis and the results of the above approximate analysis were checked. The Fourier analysis gave rise to carrier and sideband terms as shown in the spectrum of Fig. 8(a). This spectrum was experimentally checked with the results as shown in Fig. 8(b). It is seen that careful consideration must be given to the frequency response of the *IM* test apparatus to properly include all prominent distortion components.

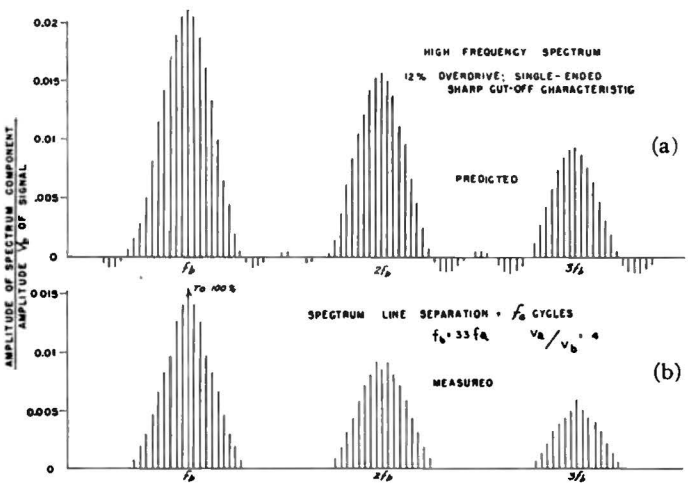

Fig. 8—Spectrum of h.f. components as found from Fourier analysis of the intermodulation products in the output of the characteristic of Fig. 6.

Fig. 9 shows the calculated and the measured values for *IM* and *HD* of the single-ended, sharp-cutoff characteristic. An average-type detector and an average-reading output meter were used, in keeping with the method of analysis. The predicted *IM* values are shown only with correction for carrier loss. The agreement with measured values is good. If the rectification characteristics of the detector and output meter are of the peak type, the *IM* results will depend upon carrier harmonic content and upon harmonics in the output voltage, as discussed below.

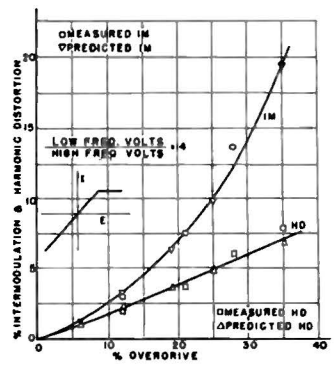

Fig. 9—Per cent intermodulation and harmonic distortion for a single-ended, sharp-cutoff characteristic as a function of overdrive.

Case (II-b). Double-Ended, Sharp-Cutoff Characteristic: Examination of the relative phase relationships of sideband components in the deficiency spectrum of Fig. 8(a) reveals that, for the push-pull, sharp-cutoff characteristic, certain carrier and sideband terms will cancel, while others will add. Taking these effects into account, it was possible to predict per cent *IM* values from

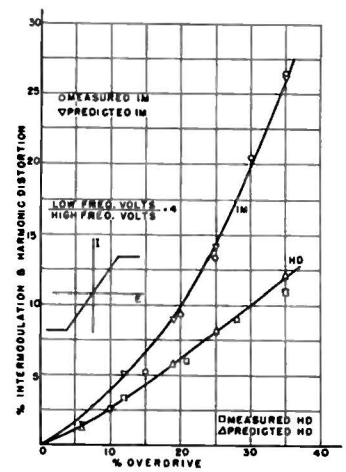

Fig. 10—Per cent intermodulation and harmonic distortion for a push-pull, sharp-cutoff characteristic as a function of overdrive.

TABLE I

4-TO-1 SIGNAL RATIO CASE; MULTIPLYING COEFFICIENTS FOR EVALUATING INTERMODULATION PRODUCTS FROM ELEVEN EQUIDISTANT ORDINATES ON RESISTIVE LOAD LINE

Frequency	Common Multiplier	Intermodulation Products				Signal Ratio, $V_a/V_b=4$ Current Ordinate Multipliers						
		i_{+5}	i_{+4}	i_{+3}	i_{+2}	i_{+1}	i_0	i_{-1}	i_{-2}	i_{-3}	i_{-4}	i_{-5}
f_b	1/3780	207	528	−585	480	−462	0	462	−480	585	−528	−207
$2f_b$	1/7560	207	114	−1227	2292	−3234	3696	−3234	2292	−1227	114	207
Coefficients found for following sum- and difference-frequency terms will be amplitudes of *each* sideband												
$f_b \pm f_a$	1/420	23	44	−44	−16	21	−56	21	−16	−44	44	23
$f_b \pm 2f_a$	1/5040	243	352	−915	320	−518	0	518	−320	915	−352	−243
$f_b \pm 3f_a$	1/24	1	0	−3	0	2	0	2	0	−3	0	1
$f_b \pm 4f_a$	1/720	23	−32	−51	64	38	0	−38	−64	51	32	−23
$f_b \pm 5f_a$	1/45	1	−3	1	4	−2	−2	−2	4	1	−3	1

the area and deficiency spectrum data of the single-ended case. The effects of "carrier loss" were similarly taken into account. Predicted and measured results for *IM* and *IID* agreed, as shown in Fig. 10. An average-type detector was used, and the output meter M' was a full-wave average-reading meter. A supplementary experimental check showed that a peak-type detector was not subject to turnover effect, but that a half-wave peak-type output meter was so subject. These effects are in agreement with the analysis presented under the section on Metering Practice below.

Case (III). Push-Pull Sine-Form Characteristic: This case, seemingly of no more than academic interest, is presented here in summary form. The results of this analysis were found useful for correlation and a check of other analyses, as described in the next paragraph.

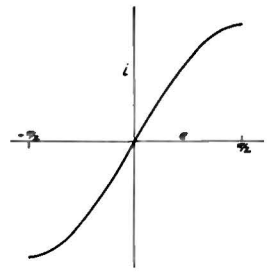

Fig. 11—Push-pull sine-form transfer characteristic.

If the transfer characteristic can be represented by a portion of a sine wave, as shown in Fig. 11, the analysis shows that, considering only the prominent sideband and harmonic terms,

$$\text{per cent } IM \cong \frac{2J_2(A)}{J_0(A)} \times 100, \tag{17}$$

and

$$\text{per cent } HD \cong \frac{J_3(A')}{J_1(A')} \times 100 \tag{18}$$

where J_0, J_1, etc., are Bessel functions of the first kind on the respective arguments, and A and A' have the same meaning as in Case (I). The theoretical ratio of *IM* to *IID* values is practically 4 for $A/B=4$ and for peak-signal levels not exceeding $e=\pi/2$. No experimental data were obtained for this case. The results serve to check those for the push-pull Case (I-b) when these results are expressed as the ratio of per cent *IM* to per cent *IID* as done in Fig. 15. *IM* values computed for the push-pull sine-form characteristic, using the coefficients listed in Tables I and II, were identical with those obtained from a more exact form of (17). This serves to check the method using these coefficients.

Effects of Metering Practice

In the intermodulation test arrangement, Fig. 1, the carrier-level meter M_c and output meter M' are generally d.c. meters used with a suitable rectifier. Each such meter-rectifier arrangement may be of the full-wave or half-wave average type, or of full-wave or half-wave peak-reading type. In general, the voltages impressed on the meter-rectifier arrangement are of complex wave form, and the readings obtained for the respective quantities will be affected by the behavior of the metering arrangement with such voltages impressed. This section summarizes analytical and experimental observations pertinent to this problem. The behavior of the full-wave and half-wave average types is the same; hence, these are referred to only as a single type in what follows.

TABLE II

1-TO-1 SIGNAL-RATIO CASE; MULTIPLYING COEFFICIENTS FOR EVALUATING INTERMODULATION PRODUCTS FROM ELEVEN EQUIDISTANT ORDINATES ON RESISTIVE LOAD LINE

Frequency	Common Multiplier	Intermodulation Products				Signal Ratio, $V_a/V_b=2/2=1$ Current Ordinate Multipliers				
		i_{+4}	i_{+3}	i_{+2}	i_{+1}	i_0	i_{-1}	i_{-2}	i_{-3}	i_{-4}
f_b	1/18	1	3	2	1	0	−1	−2	−3	−1
$2f_b$	1/24	1	2	−2	−2	2	−2	−2	2	1
$3f_b$	1/36	1	0	−4	4	0	−4	4	0	−1
Coefficients found for following sum- and difference-frequency terms will be amplitudes of *each* sideband										
$f_b \pm f_a$	1/18	1	2	1	−2	−4	−2	1	2	1
$f_b \pm 2f_a$	1/24	1	1	−2	−3	0	3	2	−1	−1
$f_b \pm 3f_a$	1/36	1	−1	−2	1	2	1	−2	−1	1
$f_b \pm 4f_a$	1/72	1	−3	2	1	0	−1	−2	3	−1

The relative phase relationships of the carrier components of voltage input to the detector in Fig. 1 are correctly given by (5). Expressed graphically, they are

as shown in Fig. 12. Certain of the harmonic components may have reversed phase if any of the coefficients

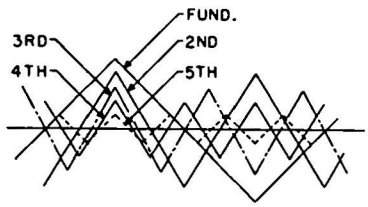

Fig. 12—Relative phase relationships of the carrier frequency and its harmonic terms from interpretation of (5). These same phase relationships apply to the l.f. components in the modulation envelopes.

a_2, a_3, etc., in (3) are negative. In general, however, the following observations pertinent to detector and metering practice in *IM* testing apply:

(a) The reading of the carrier-level meter M_c in the presence of a modulated carrier will depend upon its rectification characteristic. Thus, if the rectifier is (1) of the average type, the meter reading is unaffected by the presence of modulation and is substantially independent of the harmonic content of the signal. The area under a half cycle of a composite wave containing fundamental and 20 per cent second harmonic, with relative phase relationship as shown in Fig. 12, is hardly 2 per cent greater than the area under the fundamental alone. No turnover effect will be obtained; i.e., reversing the connections to the terminals of the meter-rectifier arrangement will not change the reading of the meter.

If the rectifier is (2) of the half-wave peak type, the meter reading will be affected by modulation and by harmonic content (magnitudes and phase relations) of the carrier. This is illustrated in Fig. 13(c), which

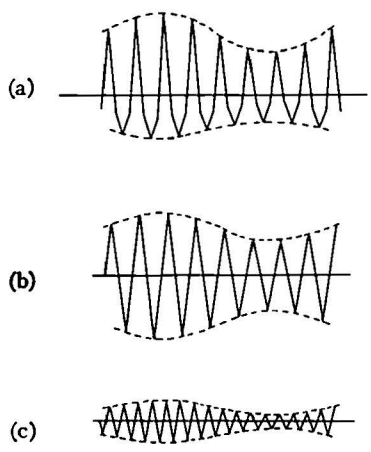

Fig. 13—Composite envelope (a), of the fundamental carrier (b) and its second harmonic (c), each of the later amplitude-modulated with the fundamental low-frequency signal.

shows the composite wave resulting from fundamental and second-harmonic carrier terms each with sideband terms corresponding to modulation at the low frequency of the test signal. This figure also indicates that turnover effect will prevail.

If the rectifier is (3) of the full-wave peak type, the meter reading will be affected by modulation and by harmonics of the carrier. There will be no turnover effect.

(b) The output of the detector will depend upon its rectification characteristic in the following ways. If the detector is (1) of the average, or "area," type, the presence of harmonics of the carrier frequency will have practically no effect on its l.f. output components. The r.m.s. summation of the sum and difference components, having frequencies $f_b \pm f_a$ and $2f_b \pm f_a$ in this instance, for a case such as developed in Fig. 13 will be almost correctly represented by the l.f. output of the average-type detector.

If the rectifier is (2) of the half-wave peak type, the output will be markedly affected by the direction of connection of the detector when harmonics of the carrier frequency combine as illustrated in Fig. 13(c) to make for different modulation-envelope amplitudes on opposite half cycles of the composite voltage.

If the rectifier is (3) of the full-wave peak type, the output will be affected by harmonics of the carrier frequency, but it will not be subject to turnover effect.

(c) The reading of the output meter M' will also be directly affected by its rectification characteristics. If the rectifier is (1) of the average type, the reading of M' will be unaffected by the direction of connection of the rectifier, and the reading will represent the r.m.s. sum of the l.f. components of a complex output voltage with good accuracy.

If the rectifier is (2) of the half-wave peak type, the reading of M' will be subject to turnover and it will be affected by the harmonic content (magnitudes and phase relations) of the output.

If the rectifier is (3) of the full-wave peak type, the reading of M' will be affected by the harmonic content (magnitudes and phase relations) of the output but will not be subject to turnover.

In summary, it follows that, depending upon their respective rectification characteristics:

(a) The carrier-meter reading may be affected by harmonics of the carrier and by the presence of modulation; (b) the detector output may be affected by harmonics of the carrier; and (c) the output-meter reading may be affected by harmonics of the l.f. (modulating) signal.

Fig. 14 shows results revealing the effect of detector and output-meter M' turnover on the per cent *IM*. These results are for the 6V6 amplifier previously treated. The tube was operated under conditions that give rise to a more prominent cubic term than indicated by (6). The solid-line curves of Fig. 14 are all for the same test-circuit conditions excepting for the output meter M' which is connected to read the average value, or positive or negative peaks. The prominent second harmonic present in the voltage being measured by the peak-type meter M' gives rise to the markedly different results for positive and negative peaks. The agreement

between per cent IM, calculated from low-frequency component voltages as measured with a harmonic analyzer, and from the full-wave average-reading meter, follows from the relative freedom of the latter from wave-form errors.

Comparison of the two center curves in Fig. 14 reveals the effect of relative phase relationship of the fundamental and second harmonic of the carrier frequency with respective first-order sidebands, as illustrated in Fig. 13. Using a half-wave peak detector to rectify the composite wave of Fig. 13(c) gives rise to a larger low-frequency component for one direction of connection of the detector than for the other. The carrier-level reading was made ahead of the detector, and a full-wave average-type meter was used. The carrier-level reading then will be independent of the direction of connection of the detector. This serves to illustrate the effect of the type and manner of connection of the detector upon per cent IM in the test arrangement considered. The effect of the detector was checked by noting that the magnitude of the f_a term, as measured with the harmonic analyzer, changed with the change in detector connection.

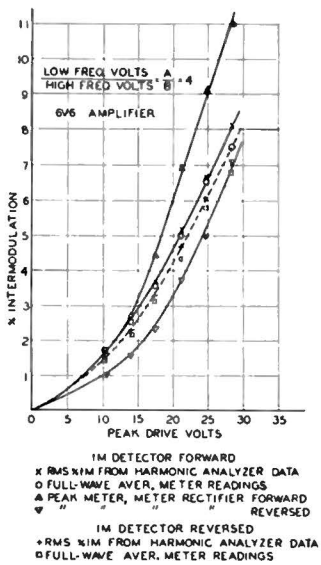

Fig. 14—Per cent intermodulation as a function of signal voltage, showing how the results are affected by direction of connection of the detector and by direction of connection and type of output meter used.

Part B—Prediction of Intermodulation Distortion

I. Approximate Prediction Equations

For amplifiers working into a resistance load, the intermodulation distortion can be predicted with the aid of equations essentially similar to those expressing harmonic distortion in terms of selected ordinates on the tube load line. Both predictions are subject to the same reservations with regard to accuracy. Using Terman's[8] method for prediction of harmonic distortion, together with the previously derived theoretical ratios of IM to HD for the signal ratio $A/B=4$, there follows:

For the single-ended amplifier, assuming only second-harmonic distortion:

$$\text{per cent } IM = 1.6\,\frac{I_{max}+I_{min}-2I_b}{I_{max}-I_{min}}\times 100. \quad (19)$$

For the push-pull amplifier, assuming only third-harmonic distortion:

$$\text{per cent } IM = 3.84\,\frac{I_{max}-I_{min}-\sqrt{2}\,(I_2-I_3)}{I_{max}-I_{min}+\sqrt{2}\,(I_2-I_3)}\times 100 \quad (20)$$

where the tube plate-current values are

I_{max} at positive peak of total signal voltage
I_{min} at negative peak of total signal voltage
I_2 at 0.707 times positive peak of total signal voltage
I_3 at 0.707 times negative peak of total signal voltage
I_b at zero signal.

II. Coefficients for Prediction from Eleven Points on Transfer Characteristic

Bloch[9] has prepared a table of multiplying factors for calculation of the amplitudes of the sideband terms from the current values on the tube load line. The tabulation is limited to a signal ratio amplitude (A/B) not greater than 3. Use of this method yields the actual current amplitudes of the sideband terms. Extension of the work of Espley[10] to enable calculation of harmonics up to the 8th from nine equally spaced ordinates made it possible to extend the tables of Bloch to the case of signal ratio=4. The fundamental and second-harmonic carrier terms and all prominent sideband terms can be calculated by use of Table I. The eleven current values, designated as i_{+5}, $i_{+4}\cdots i_0\cdots i_{-4}$, i_{-5}, are taken from the load line for corresponding, equal intervals of the total peak-signal voltage. Each current value is multiplied by the factor listed, and the sum of such products, with due regard to sign, is formed and multiplied by the common multiplier. The result will be the amplitude, in current units, of the corresponding carrier or sideband term. As an example, the following are the results for the triode-connected 6V6 of Case I-a; signal ratio $A/B=4$, 20 volts peak drive, and 26 volts bias:

Instantaneous grid voltage	Plate-current (ma.)
− 6	53.0
−10	48.7
−14	44.6
−18	40.7
−22	36.9
−26	33.2
−30	29.5
−34	25.9
−38	22.4
−42	18.9
−46	15.5

[8] See p. 380 of footnote reference 7.

[9] A. Bloch, "Modulation products; calculation from equidistant ordinates," *Wireless Eng.*, vol. 23, pp. 227–230; August, 1946.

[10] D. C. Espley, "The calculation of harmonic production in thermionic valves with resistive loads," Proc. I.R.E., vol. 21, pp. 1439–1446; October, 1933.

Use of the tabulated multipliers yields:

Current of frequency $f_b = 3.755$ ma.

Current of frequencies $f_b \pm f_a = 0.170$ ma.

Current of frequencies $f_b \pm 2f_a = 0.021$ ma.

Current of frequency $2f_b = 0.039$ ma.

Per cent $IM \cong (2 \times 0.170/3.755) \times 100 = 9.1$ per cent.

When testing the performance of amplifiers at the higher frequencies, it is sometimes found desirable to use a signal ratio of 1. Table II gives the multipliers for predetermining the carrier frequency and sideband terms for this signal ratio.

Conclusions

I. If the transfer characteristic of a network is substantially independent of frequency, it is possible to evaluate the intermodulation and harmonic distortion due to the nonlinearity of the characteristic. Relatively simple equations are derived for per cent IM and per cent HD for transfer characteristics expressible in simple analytic form.

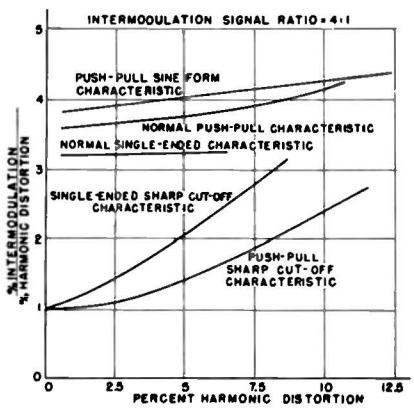

Fig. 15—Ratio of intermodulation to harmonic distortion as a function of the latter for some typical transfer characteristics. The intermodulation test method for which these results apply is described in the text of this paper.

For a given intermodulation test method, therefore, the specified operating conditions can be introduced to uniquely evaluate this distortion. It becomes possible, then, to express the ratio of the two distortion percentages. This has been done for certain typical transfer characteristics and for an intermodulation test method as described, and the ratios have been found to be relatively constant. Fig. 15 summarizes these ratios for the cases covered by this study.

II. The presently accepted value of 4:1 for ratio of signal amplitudes in intermodulation testing is a good compromise, making for operating conditions that give a high IM percentage and still have reasonable values of carrier and sideband voltages for detection and measurement.

III. The type of carrier-level meter, detector, and output meter used in the intermodulation testing apparatus will each, and in combination, affect the results obtained.

The analysis above indicates that the intermodulation-measurement technique will best satisfy the defining equation if an average-type detector is used and if the carrier-level and output meters are of the average-reading type. This practice will also help eliminate differences that may appear in IM results obtained with apparatus of different manufacture in which different amounts of phase shift are introduced between the fundamental and harmonics. Such phase shift differences will have a direct bearing upon the output of a peak-type detector as well as upon the readings of peak-type meters.

IV. Intermodulation-distortion percentage values are readily predictable from transfer characteristic or load-line data by the use of tabulated multiplying coefficients that can be used to calculate the magnitudes of the usually prominent intermodulation terms.

Automatic Volume Control as a Feedback Problem*

B. M. OLIVER†, MEMBER, I.R.E.

Summary.—**Feedback amplifier theory is shown to be applicable to the usual a.v.c. system. Expressions are derived for the loop gain in terms of the design requirements and the gain-control characteristic of the controlled amplifier. Using these expressions, the design of an a.v.c. system is quite straightforward, and its characteristics, such as regulation and effect on desired modulation, are readily predictable.**

* Decimal classification: R361.201 × R139.2. Original manuscript received by the Institute, July 8, 1946; revised manuscript received, October 8, 1947.

† Bell Telephone Laboratories, Inc., New York, N. Y.

I. Introduction

A SIMPLE FEEDBACK amplifier has these essential features:

(1) There is an input.

(2) There is an output.

(3) There is a transmission path (called the β circuit) which develops a measure of the output.

(4) There is a means for comparing this measure of the output with the input, i.e., means for developing a "net" or "error" signal which is the algebraic sum of the input and the measure of the output.